Available online at www.sciencedirect.com
ScienceDirect
Cement and Concrete Research 37 (2007) 21–31
Cement and Concrete Research

Structure and phase investigations on crystallization of 11 Å tobermorite in lime sand pellets☆

A. Hartmann [a,*], J.-Ch. Buhl [b], K. van Breugel [a]

[a] Materials Science Section, Faculty of Civil Engineering and Geosciences, Delft University of Technology, 2628 CN, Delft, The Netherlands
[b] Institute of Mineralogy, University Hannover, D-30167 Hannover, Germany

Received 28 February 2005; accepted 18 September 2006

Abstract

The present work examines the crystallization behaviour of 11 Å tobermorite and its dependence on the reactivity of different silica sources (quartz sand, grain-size ≤0.30 mm; quartz powder, grain-size ≤0.08 mm; inflated clay sand, grain-size ≤0.50 mm and raw perlite, grain-size ≤1 mm). The influence of different C/S ratios (calcium/silica ratio: 0.53, 0.83) was also investigated. For simulation of the industrial production process of lime sand products, a synthesis of lime sand pellets was carried out with a hydrothermal treatment (T=200 °C, t=40.5 h). The C–S–H phases were characterized by ESEM, EDX and X-ray powder diffraction.

The investigations revealed that the grain-size, C/S ratio and porosity of the silica sources influence the formation of 11 Å tobermorite. A formation of 11 Å tobermorite using inflated clay sand with a grain-size ≤0.50 mm and a high porosity was only found with a C/S ratio of 0.53. This indicates a negative influence of an increase of lime content inside the synthesis mixture for tobermorite crystallization.

Besides, a formation of xonotlite inside big pores of the lime sand pellet with inflated clay sand could be observed. The formation of portlandite and calcite was detected in all samples. The amount of calcite increased with the grain-size and with a higher C/S ratio.

Keywords: Calcium–silicate–hydrate (C–S–H); Hydration product; SEM; EDX; X-ray diffraction

1. Introduction

In commercial lime sand products a reaction of a mixture of quartz, lime hydrate and water takes place under hydrothermal conditions. During this reaction calcium–silicate–hydrate phases (C–S–H phases) are formed. The stability of lime sand products is based on the formation of C–S–H phases because they are the binding agents for the cementing of the quartz. Under common reaction conditions of 180–200 °C and a water vapour pressure of 16 bar the formation of 11 Å tobermorite as the main C–S–H phase takes place [1]. The development of high-tech-products needs more basic mineralogical research to optimize important properties, such as the stability of lime sand products. This includes investigations concerning the crystallization and the morphology of C–S–H phases such as 11 Å tobermorite under different reaction conditions. Whereas in our former investigations hydrothermal syntheses were performed on powder samples [2–4], the present work simulates the industrial production of lime sand products [5]. Pellets, prepared from different silica sources, were used for hydrothermal synthesis. The pellets were investigated by Environmental Scanning Electron Microscopy (ESEM), Energy Dispersive X-ray analysis (EDX analysis) and X-ray powder diffraction (XRD). Additionally on selected lime sand pellets the porosity was determined to investigate its relation to the structure and the amount of C–S–H phases within the pellets.

The different silica sources, used for pellet preparation, were included in the experimental investigations. To examine their chemical composition and to check the reactivity the silica sources were investigated by ESEM and EDX analysis.

2. Materials and methods

2.1. Raw materials for preparation of lime sand pellets

The silica sources used for the preparation of the lime sand pellets are summarized in Table 1. These are the same materials

☆ *In memorium Ch. F. Hendriks.*

* Corresponding author. Tel.: +49 163 1545 744; fax: +31 15 278 8162.
E-mail address: a.hartmann@tudelft.nl (A. Hartmann).

0008-8846/$ - see front matter © 2006 Elsevier Ltd. All rights reserved.
doi:10.1016/j.cemconres.2006.09.007

Table 1
Overview of used silica sources for preparation of lime sand pellets

Nr.	Silica source	Origin
1	Quartz sand	Research communication "Kalk-Sand e.V., Hannover"
2	Quartz powder	FLUKA CHEMIKA 83340, p.a. powder
3	Inflated clay sand	Dansk Leca
4	Raw perlite	Heidelberger Zement AG

as were used in our previous syntheses of powder samples [2–4].

The lime used was calcinated $CaCO_3$ (1000 °C for 3 h) from JOHNSON Matthey GmbH [2–4].

2.2. Preparation of lime sand pellets

For the preparation of lime sand pellets the respective silica and calcium sources were weighed to provide C/S ratios of 0.53 and 0.83 and were mixed with 20 ml distilled water to a homogeneous suspension. The 0.53 ratio had been found to be the favoured ratio with powder samples and was used here to allow a comparison of the experimental results [2,3]. Literature research [6–13] gives a C/S ratio of 0.83 to be the favoured ratio for the crystallization of 11 Å tobermorite.

The lime sand pellets were pressed at a pressure of 5 kg/m^2 for about 3 min. The lime sand pellets had an average diameter of 1 cm and an average height of 0.50 cm.

2.3. Reaction conditions of vapour hardening

The synthesis of lime sand pellets was carried put in a Berghof-Toelg steel autoclave under hydrothermal conditions. As reaction vessel a PTFE (polytetrafluoroethylene) inlay with a volume of 50 ml, closed with a cap, was used. Inside this cap a special PTFE sieve inlay was screwed in, where the pellets were positioned. The distance between the sieve inlay and the hydrothermal liquid (20 ml dist. water) was about 3 cm. In contrast to the synthesis of powder samples in this case there was no direct contact between the pellet and the hydrothermal liquid. The synthesis resulted only from the vapour pressure of water, which was built up in the PTFE inlay during the experiment. A reaction temperature of 200 °C and a reaction time of 40.5 h were used.

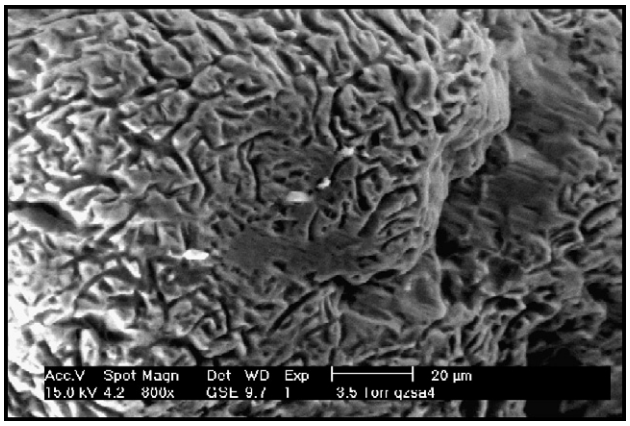

Fig. 1. ESEM image of quartz sand.

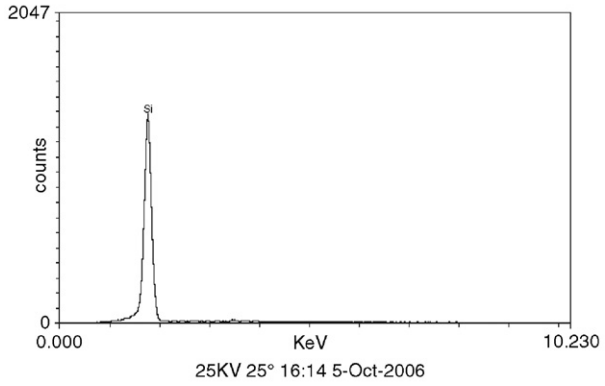

Fig. 2. EDX spectrum of quartz sand.

2.4. Investigation methods

The electron microscopical investigations of the silica sources and lime sand pellets were done with a Philips XL 30 ESEM. Here a secondary electron image (SE) under a water vapour atmosphere at a pressure of 3.5 Torr is possible using a GSE Detector (Gaseous Secondary Electron Detector). The acceleration voltage was 15 kV. The determination of the element concentration of the silica sources and the C–S–H phases was done by EDX analysis.

The qualitative phase analysis of the different binding agent materials of the lime sand pellets was carried out by X-ray powder diffraction (Phillips PW 1800, with CuKα radiation). A small amount of sample material was removed from the quartz grains of the pellets using a 35 µm sieve of V2A-steel. The samples were investigated at the University Hannover. The 2-Theta values ranged from 5° to 80° and were recorded in 0.02° steps with a counting time of 4 s per step. For the phase analysis of the lime sand pellets WINX POW (Company Stoe) was used.

Porosity and pore radius distribution were determined on selected lime sand pellets with an Hg-pressure porosimeter (type Micromeritics Pore Sizer 9320), Delft University of Technology.

3. Interpretation of the results

3.1. ESEM/EDX results of the silica sources

The quartz sand showed a rough and strongly fissured surface of the quartz grains (grain-size ≤0.30 mm). The single grains have different shapes and are partially rounded (Fig. 1).

Table 2
Element amount [in weight %] of the silica sources

Source	O	Si	Ca	Na	Mg	Al	K	Fe
Quartz sand	46.5	36.6	16.9	–	–	–	–	–
Quartz powder	48.1	51.9	–	–	–	–	–	–
Inflated clay sand	41.4	26.8	2.3	1.5	2.7	12.5	2.9	9.9
Raw perlite	50.7	33.7	1.0	1.9	0.7	7.5	3.0	1.5

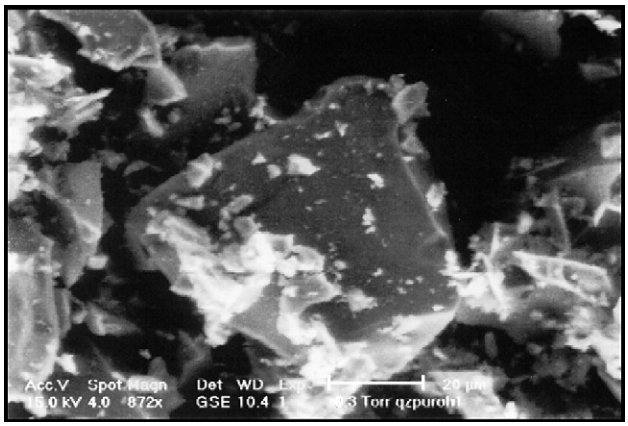

Fig. 3. ESEM image of quartz powder.

The EDX spectrum of quartz sand shows an amount of O and Si, given in Fig. 2. The amount of C refers to bituminous pollution. The element amount in weight % is given in Table 2.

The quartz powder (grain-size ≤0.08 mm) showed a smooth surface and a platy morphology of the single quartz grains (Fig. 3). The EDX spectrum of quartz powder shows peaks of Si and O (Fig. 4). In Table 2 the element amount in weight % is given.

The single inflated clay grains (grain-size ≤0.50 mm) show a high porosity (Fig. 5). The average pore size could be specified with 1 μm. The EDX spectrum of an inflated clay grain shows besides an amount of O and Si also peaks of Fe, Mg, K, Al, Ca and Na, Fig. 6. This refers to the amount of clay minerals in the inflated clay sand [10]. These elements are called "foreign elements" in production of lime sand materials and their influence on C–S–H phase formation is not yet clear up to now. In Table 2 the element amount in weight % is given.

The single raw perlite grains (grain-size ≤1 mm) show a smooth, partly fissured surface (Fig. 7).

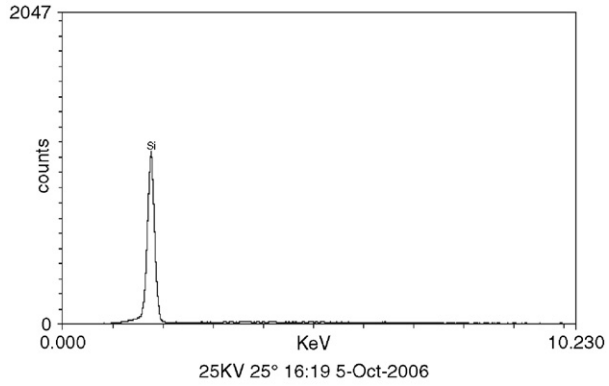

Fig. 4. EDX spectrum of quartz powder.

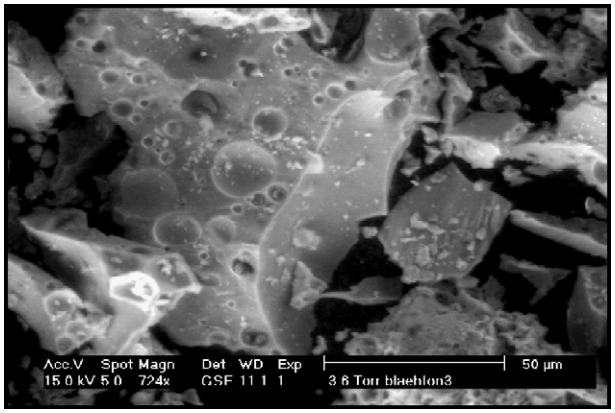

Fig. 5. ESEM image of inflated clay.

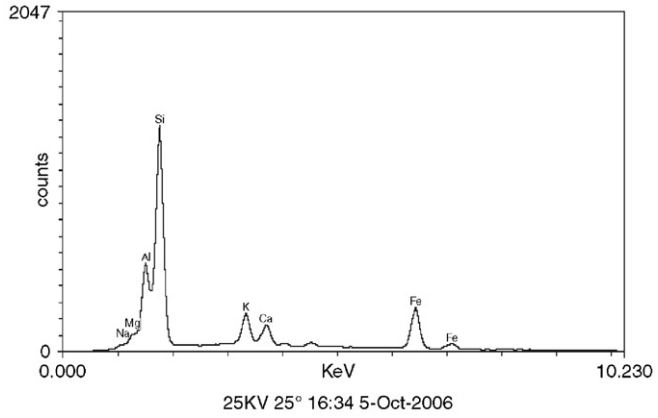

Fig. 6. EDX spectrum of inflated clay.

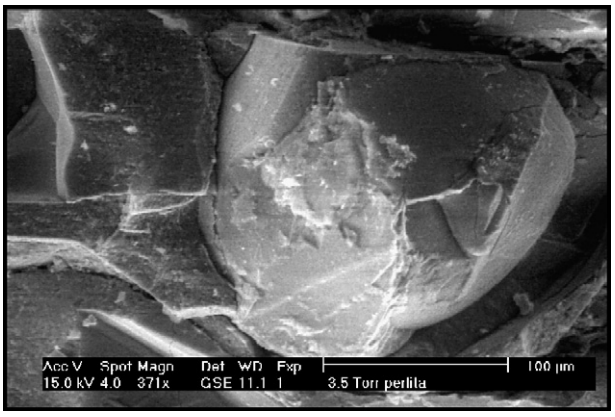

Fig. 7. ESEM image of raw perlite.

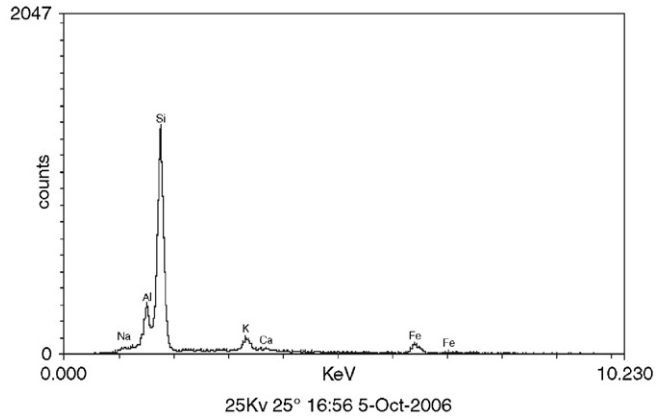

Fig. 8. EDX spectrum of raw perlite.

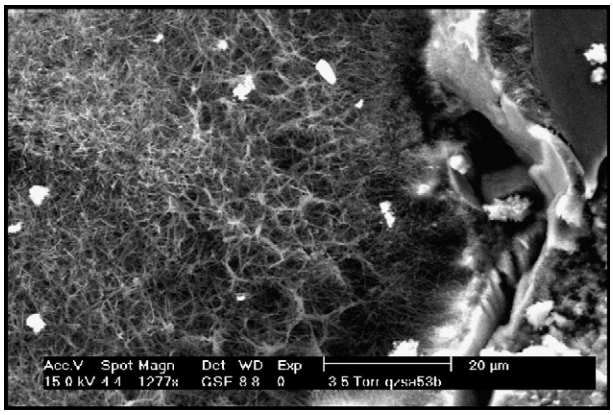

Fig. 9. ESEM image of lime sand pellet with quartz sand (C/S=0.53).

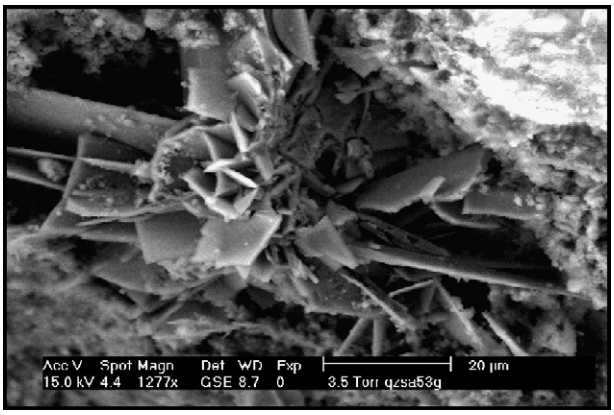

Fig. 10. ESEM image of lime sand pellet with quartz sand (C/S=0.53).

The element distribution of the raw perlite is given in the EDX spectrum with peaks of O, Si and also an amount of the "foreign elements" Fe, K, Mg, Al, Ca and Na (Fig. 8). Table 2 shows the element amount in weight %.

3.2. ESEM/EDX results of the lime sand pellets (C/S=0.53/0.83) after vapour hardening

3.2.1. Pellets with quartz sand

In the lime sand pellet with quartz sand and a C/S ratio of 0.53 the individual quartz grains lay in a matrix of $Ca(OH)_2$. Between the single quartz grains cavities with an average size of about 10 µm could be observed. The quartz grains showed partial dissolution at the rims with simultaneous formation of C–S–H phases. Some of the quartz sand grains are covered by a "cobweb-like" C–S–H layer (Fig. 9), termed as C–S–H (I) [1]. The EDX analysis in weight % is given in Table 3. Between the quartz grains some larger cavities up to 100 µm could be observed, in which platy C–S–H crystals with a maximum size of 40 µm had been formed (Fig. 10). These crystals could be identified as α-C_2SH from the X-ray powder diffraction results, given below. The EDX analysis in weight % is shown in Table 3.

In analogy to the synthesis with a C/S ratio of 0.53 the quartz sand grains in the pellet with a C/S ratio of 0.83 lay in a matrix of $Ca(OH)_2$. In contrast to the C/S ratio of 0.53 the single grains here showed an only weak dissolution of the rims. The surface was only partly dissolved. Compared to the pellet with a C/S ratio of 0.53 only a small amount of C–S–H phases could be observed. The cavities between the quartz grains with a maximum size of 5 µm in most cases showed no formation of C–S–H phases, as can be seen from Fig. 11. The element amount in weight % is given in Table 3.

Fig. 11. ESEM image of lime sand pellet with quartz sand (C/S=0.83).

3.2.2. Pellets with quartz powder

In the lime sand pellets with quartz powder and a C/S ratio of 0.53 the single quartz grains as well were embedded in a Ca $(OH)_2$ matrix. Between the single quartz grains some cavities

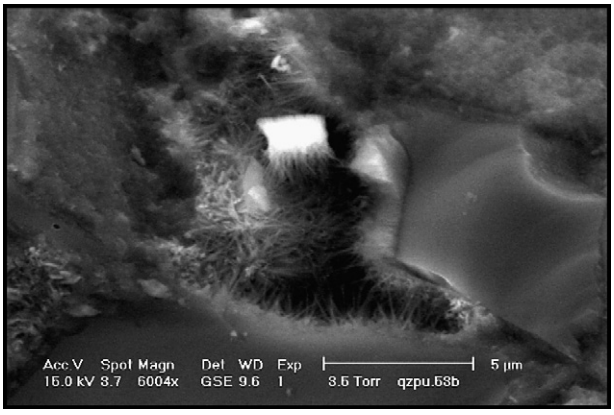

Fig. 12. ESEM image of lime sand pellet with quartz powder (C/S=0.53).

Table 3
Element amount [in weight %] of the reaction products with C/S=0.53 and C/S=0.83

Source	O	Si	Ca	Na	Mg	Al	K	Fe
Quartz sand (C/S=0.53)	50.7	16.2	33.1	–	–	–	–	–
Quartz sand (C/S=0.53)	47.0	18.5	34.5	–	–	–	–	–
Quartz sand (C/S=0.83)	48.1	28.4	23.5	–	–	–	–	–
Quartz powder (C/S=0.53)	43.5	25.4	31.1	–	–	–	–	–
Quartz powder (C/S=0.83)	43.5	25.4	31.1	–	–	–	–	–
Inflated clay sand (C/S=0.53)	36.3	14.3	21.1	0.4	0.9	5.3	2.1	4.2
Inflated clay sand (C/S=0.83)	36.2	21.3	8.9	0.6	1.8	9.2	3.3	18.7

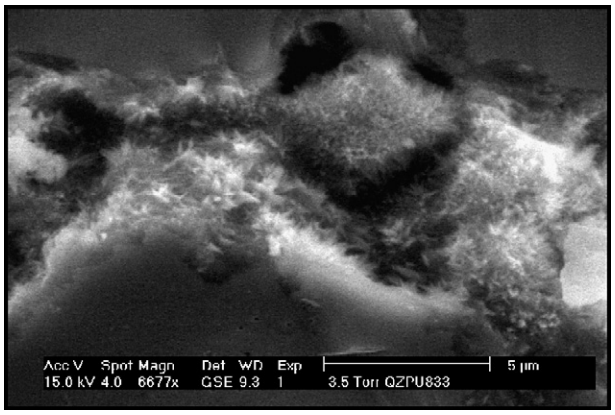

Fig. 13. ESEM image of lime sand pellet with quartz powder (C/S=0.83).

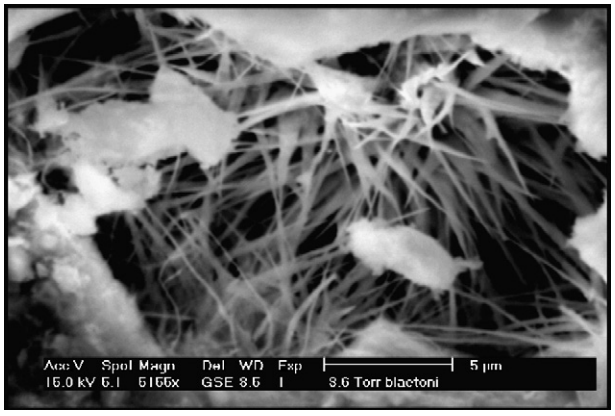

Fig. 14. ESEM image of lime sand pellet with inflated clay sand (C/S=0.53).

with an average size of 3 µm have developed. At the grain rims the formation of gel-like sheets of C–S–H phases with a maximum thickness of 5 µm could be observed. From these sheets single needle-like C–S–H phases with a size of ≤2.5 µm have developed growing into the cavities, Fig. 12. The EDX analysis in weight % is shown in Table 3.

For C/S=0.83 the quartz powder grains are also well embedded in a matrix of $Ca(OH)_2$. The grain rims exhibit dissolution patterns with a formation of C–S–H phases. In

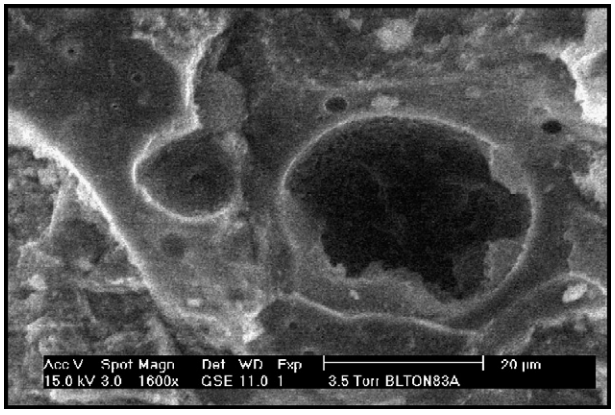

Fig. 15. ESEM image of lime sand pellet with inflated clay sand (C/S=0.83).

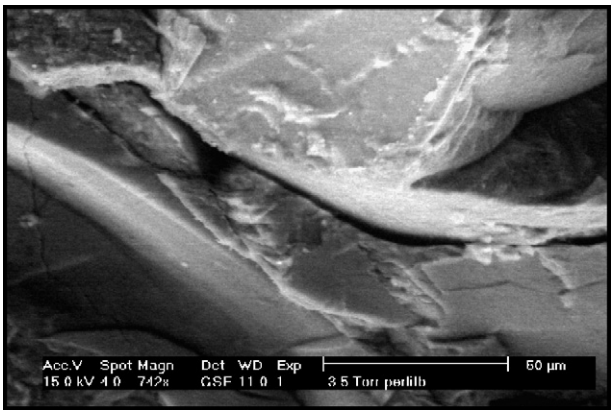

Fig. 16. ESEM image of lime sand pellet with raw perlite (C/S=0.53).

contrast to the lime sand pellet with a C/S ratio of 0.53 no fine C–S–H needles could be found, but C–S–H reaction zones with a maximum thickness of 3 µm. They fill the cavities (maximum size 5 µm), as seen in Fig. 13. An EDX analysis in weight % is given in Table 3.

3.2.3. Pellets with inflated clay sand

The porosity of the lime sand pellets with inflated clay sand is similar to the pure inflated clay sand grains. The reaction with Ca

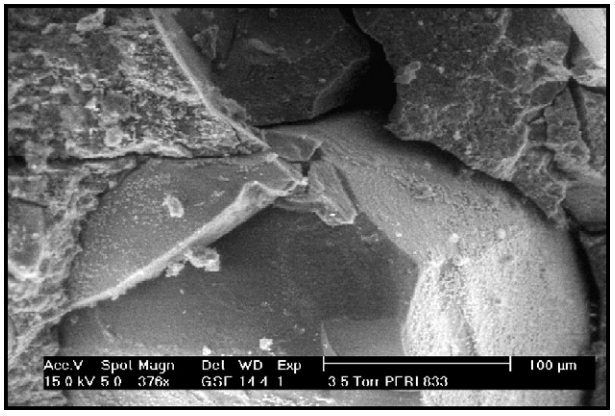

Fig. 17. ESEM image of lime sand pellet with raw perlite (C/S=0.83).

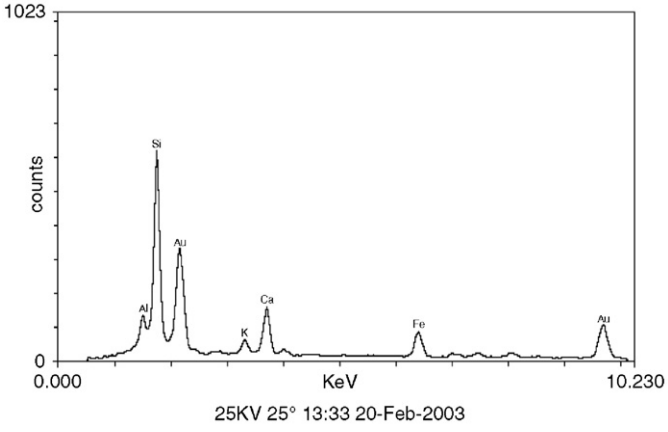

Fig. 18. EDX spectrum of lime sand pellet with raw perlite (C/S=0.53).

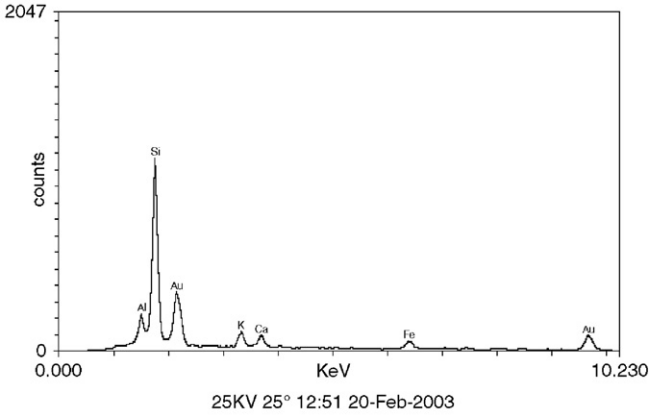

Fig. 19. EDX spectrum of lime sand pellet with raw perlite (C/S = 0.83).

$(OH)_2$ took place abundantly at the pore edges of the inflated clay grains with a C/S ratio of 0.53. Additionally, pores of up to 30 μm developed. In some of these pores needle-like C–S–H phases with a maximum size of 10 μm could be observed (Fig. 14). Because of the large crystal size, a formation of xonotlite can be supposed [6]. The EDX analysis in weight % is given in Table 3.

The results of the present experiments illustrate that a formation of xonotlite was also possible in the presence of "foreign elements" such as Al, Fe, K, Mg and Na. The morphology of xonotlite was not influenced by these elements.

With a C/S ratio of 0.83 the pores showed an average maximum size of 20 μm. In contrast to the pellet with a C/S ratio of 0.53 no formation of needle-like C–S–H phases took place inside the pores. At the edges of the pores only the beginning of the formation of gel-like C–S–H phases could be observed (Fig. 15). The EDX analysis in weight % is given in Table 3. The results show that an increase of the C/S ratio influences the morphology of the developed C–S–H phases. Instead of needle-like crystals gel-like material occurs.

3.2.4. Pellets with raw perlite

Because of technical problems at the ESEM at the Delft University of Technology the electron microscopical and EDX investigations of the pellets with raw perlite were done at the University Hannover. Here a SEM Hitachi S-530 was used. Before the pellets could be investigated by the SEM, the samples had to be covered with a gold layer to prevent sample charging, so a gold peak is seen in the EDX spectrum (Figs. 18 and 19).

In the lime sand pellets with raw perlite no formation of C–S–H phases could be observed for either C/S ratio (Figs. 16 and 17). Cavities of up to 5 μm between the raw perlite grains were free of reaction products. An EDX analysis of a raw perlite grain in the pellet with a C/S ratio of 0.53 showed peaks of Si, Ca, Fe, K and Al. Compared to the Si peak the Ca peak shows a lower intensity (Fig. 18).

The EDX analysis of a raw perlite grain of the pellet with a C/S ratio of 0.83 again shows a Ca peak with low intensity compared to the higher intensity Si peak (Fig. 19).

In contrast XRD gave evidence for CSH I and α-C_2SH formation. Thus these products seem to be very thin crystalline covers around the surface of the perlite grains and ESEM resolution as well as EDX analysis seems to be disturbed by charge effects of the sample as well as strong background excitation effects.

3.3. XRD results

3.3.1. Pellets with quartz sand

The X-ray powder patterns of the lime sand pellets with quartz sand and C/S ratios of 0.53 (Fig. 20) and 0.83 (Fig. 21) showed distinct peaks of quartz [PDF-No. 5–490], α-C_2SH [PDF-No. 9–325], C–S–H (I) [PDF-No. 9–210], portlandite [PDF-No. 4–0733] and calcite [PDF-No. 5–586]. The increase of the C/S ratio from 0.53 to 0.83 was characterized by a distinct increase of the peak intensities of the C–S–H (I) and, especially, the portlandite and calcite peaks.

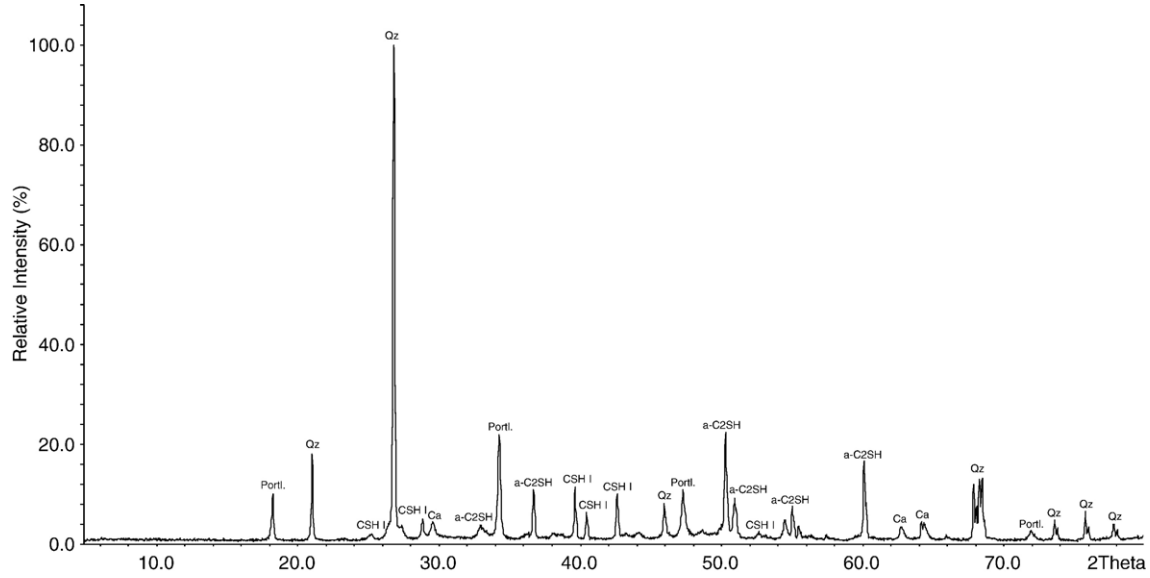

Fig. 20. X-ray powder pattern of the lime sand pellet with quartz sand (C/S = 0.53).

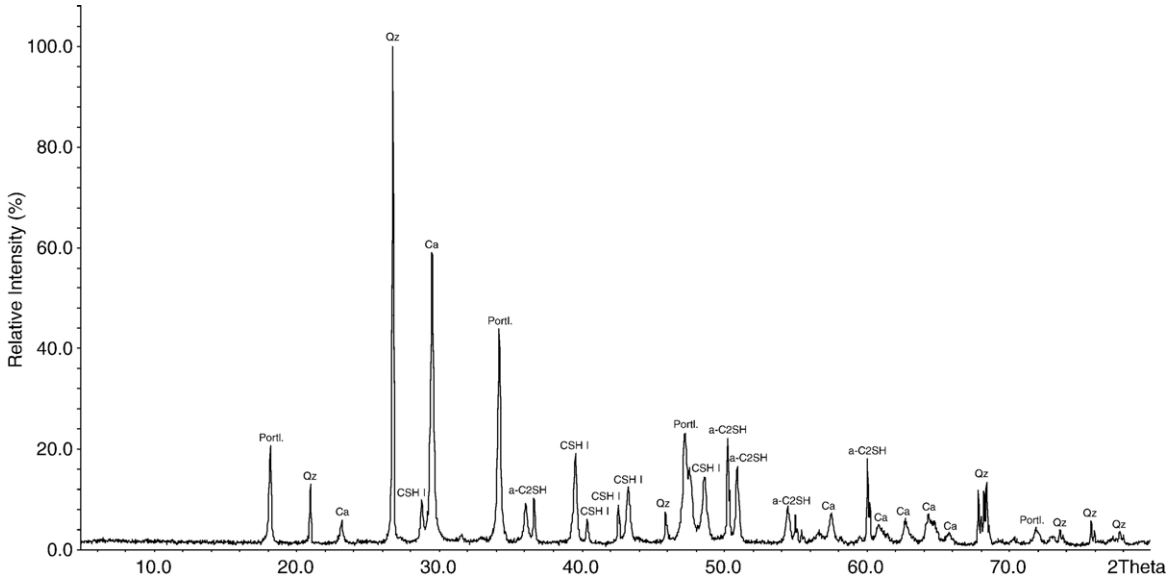

Fig. 21. X-ray powder pattern of the lime sand pellet with quartz sand (C/S = 0.83).

In the X-ray powder pattern of the lime sand pellet with quartz sand no 11 Å tobermorite [PDF-No. 10–373] peak could be identified in the pellets of both C/S ratios.

3.2. Pellets with quartz powder

The X-ray powder patterns of the lime sand pellets with quartz powder and C/S ratios of 0.53 (Fig. 22) and 0.83 (Fig. 23) showed peaks of quartz, α-C_2SH, C–S–H (I), portlandite and calcite. For a C/S ratio of 0.83, higher portlandite reflection intensities were observed than for the pellet with a C/S ratio of 0.53. A formation of 11 Å tobermorite could not be identified from the powder pattern of the lime sand pellets with quartz powder for either C/S ratio.

3.3. Pellets with inflated clay sand

The X-ray powder pattern of the lime sand pellet with inflated clay sand and a C/S ratio of 0.53 (Fig. 24) showed a high background, indicating amorphous material. Crystalline phases were also present, represented by distinct peaks. They could be identified as quartz, α-C_2SH, C–S–H (I), portlandite and calcite. In contrast to the results presented so far, a formation of 11 Å tobermorite and xonotlite could be verified from weak reflections of tobermorite and somewhat more intense ones for xonotlite. In the case of the formation of xonotlite these results agree with the ESEM investigation (see Section 3.2.3).

The X-ray powder pattern of the lime sand pellets with inflated clay sand and a C/S ratio of 0.83 (Fig. 25) shows no

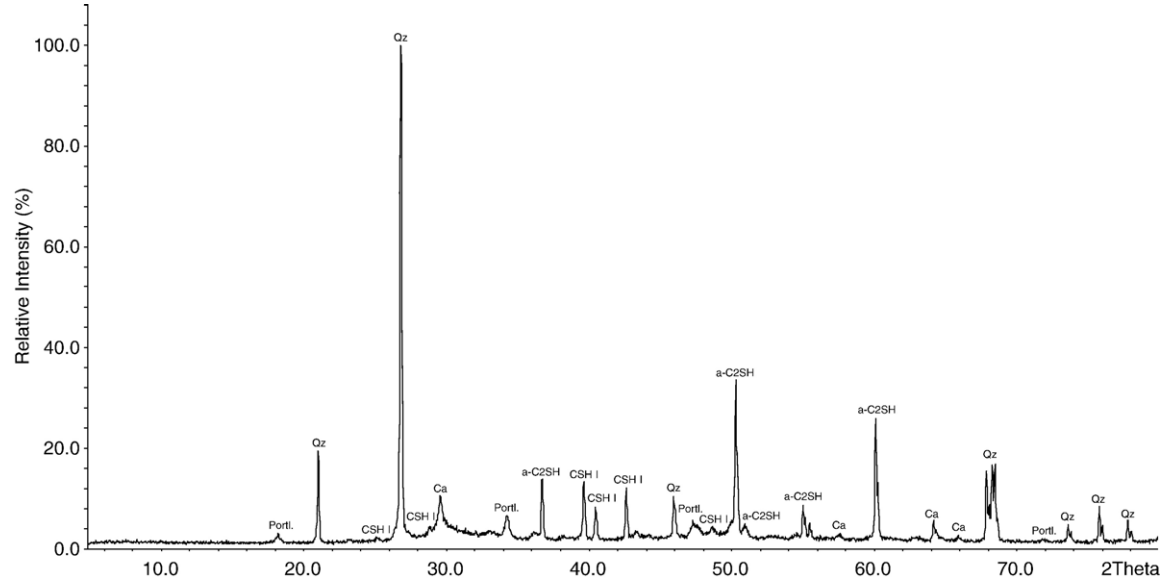

Fig. 22. X-ray powder pattern of the lime sand pellet with quartz powder (C/S = 0.53).

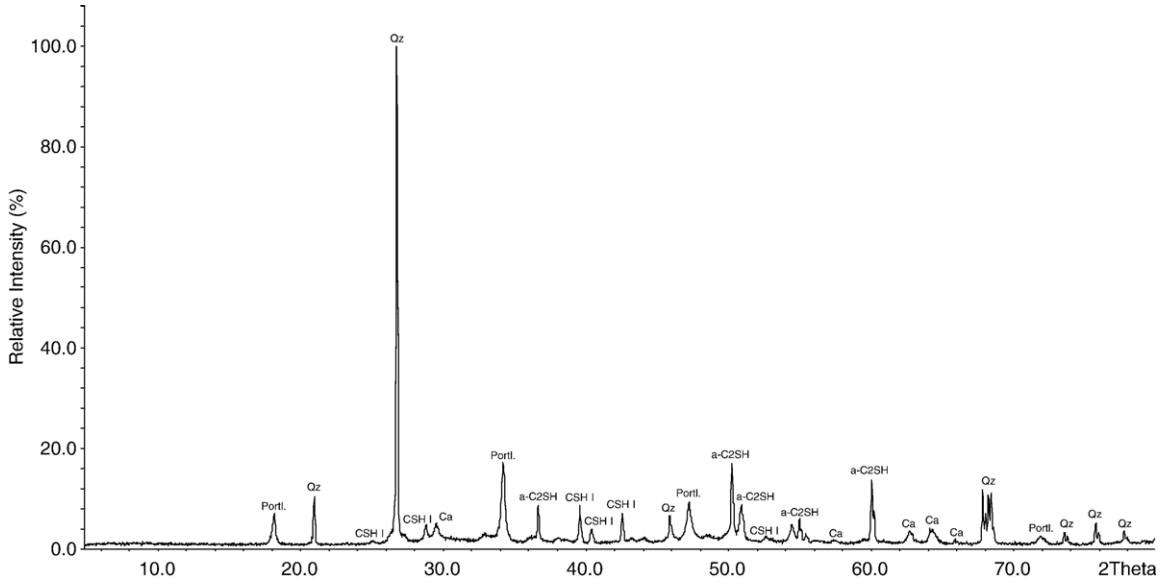

Fig. 23. X-ray powder pattern of the lime sand pellets with quartz powder (C/S = 0.83).

11 Å tobermorite peak and only a xonotlite peak with weak intensity. This also agrees with the results of the ESEM investigation (see Section 3.2.3). In analogy to the results presented so far, the portlandite peaks increased in intensity from a C/S ratio of 0.53 to 0.83.

3.4. Pellets with raw perlite

In the X-ray powder pattern of the lime sand pellets with raw perlite distinct peaks of α-C_2SH, C–S–H (I), portlandite and calcite could be identified for both C/S ratios (Figs. 26 and 27). The powder pattern for a C/S ratio of 0.53 showed a higher background besides quartz peaks of high intensity. No differences in the intensity of the portlandite peaks could be detected for either C/S ratio. In agreement with the ESEM investigation 11 Å tobermorite could not be identified for either ratio.

3.4. Results of the Hg-porosity on selected lime sand pellets (C/S = 0.53)

In Table 4 the values of the pore area [m^2/g], the pore diameter [μm] and the porosity [%] of the lime sand pellets with quartz powder, quartz sand, inflated clay sand and raw perlite are given for the samples with a C/S ratio of 0.53.

The lime sand pellet with inflated clay sand has the highest pore area compared to pellets with quartz powder, quartz sand or raw perlite. The porosity of the lime sand pellets with inflated clay sand was distinctly higher than the porosity of the lime sand pellets with quartz powder, quartz sand or raw perlite. This agreed with the results of the ESEM investigation of the lime sand pellets (see Section 3.2). Here the lime sand pellet with inflated clay sand and a C/S ratio of 0.53 also showed a distinct

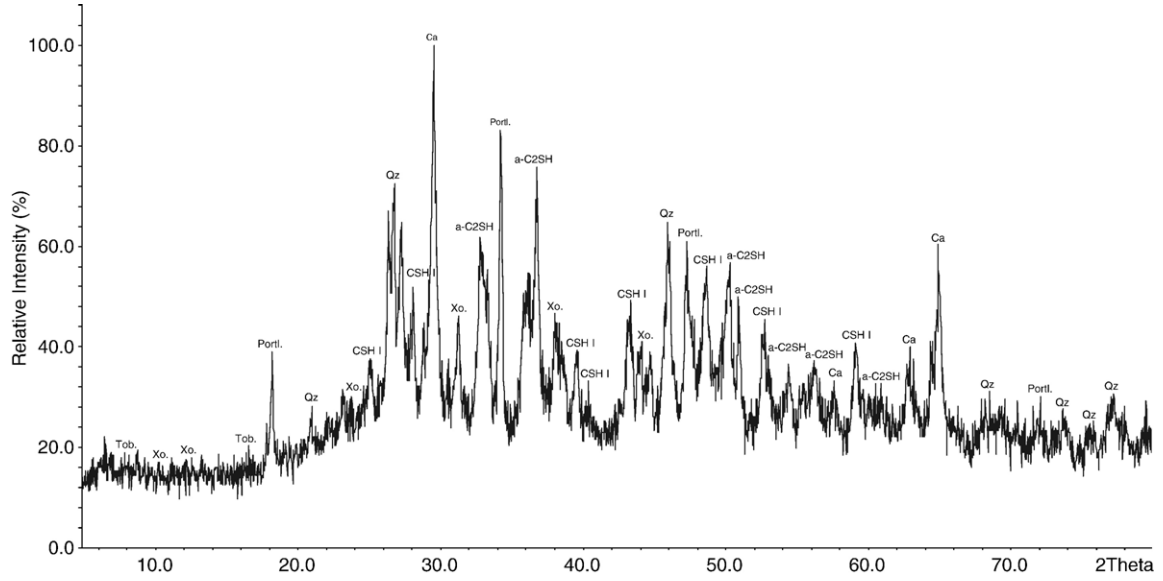

Fig. 24. X-ray powder pattern of the lime sand pellet with inflated clay sand (C/S = 0.53).

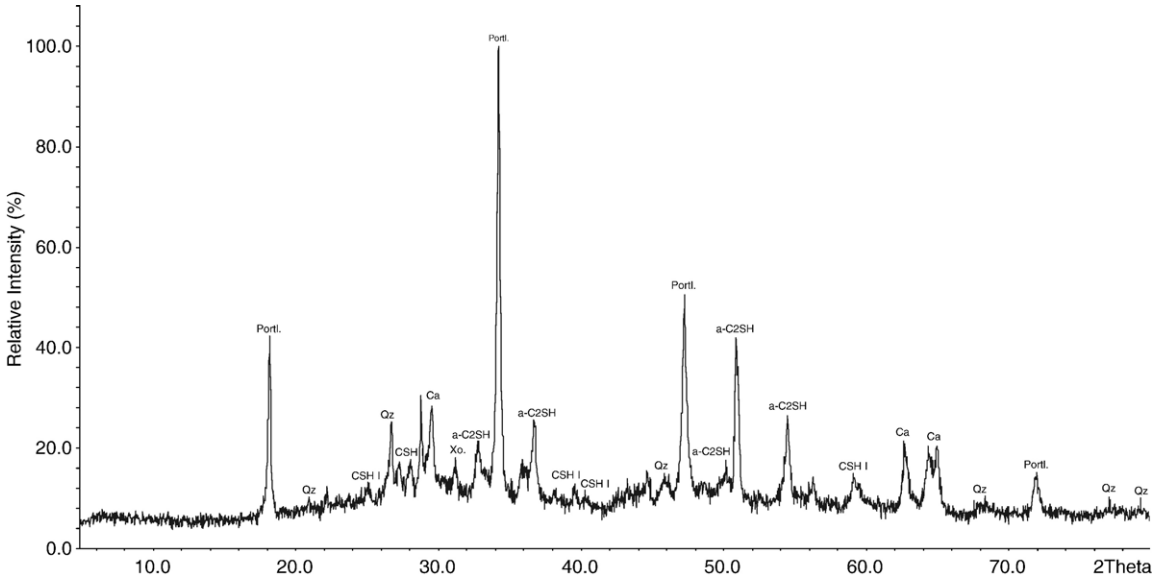

Fig. 25. X-ray powder pattern of the lime sand pellet with inflated clay sand (C/S = 0.83).

porosity in contrast to the lime sand pellets with quartz powder, quartz sand or raw perlite. The average pore diameter was lowest for the lime sand pellet with inflated clay sand. Distinctly higher values were found for the lime sand pellets with quartz powder, quartz sand and raw perlite. Overall, the lime sand pellet with quartz sand had the lowest porosity and the highest average pore diameter.

4. Discussion

The lime sand pellet with quartz sand and a C/S ratio of 0.53 was found to be not very compact: the texture of the pellet was characterized by cavities with a size of ≤ 10 μm. Between the quartz grains large C–S–H (I) sheets could be observed. A cementation of the quartz grains through the formation of 11 Å tobermorite could not be verified by ESEM, and X-ray analysis did not detect 11 Å tobermorite in these pellets. ESEM investigations revealed the formation of C–S–H (I) besides the formation of platy crystals of α-C_2SH with a maximum size of 40 μm. These crystals occurred in cavities with a size of ≤ 100 μm. The formation of platy crystals in spacious cavities between the quartz grains was also observed by [7]. X-ray analysis revealed α-C_2SH, C–S–H (I) and portlandite as reaction products. The formation of calcite could be verified by X-ray investigation only, whereas the ESEM detected no calcite. Investigations by [9] on conventional powder samples showed that α-C_2SH appears as the first reaction product when using silica with a grain-size of 0.10–1 mm. Here the amount of residual quartz also could be determined. The results of the present work on vapour hardened lime sand pellets with quartz

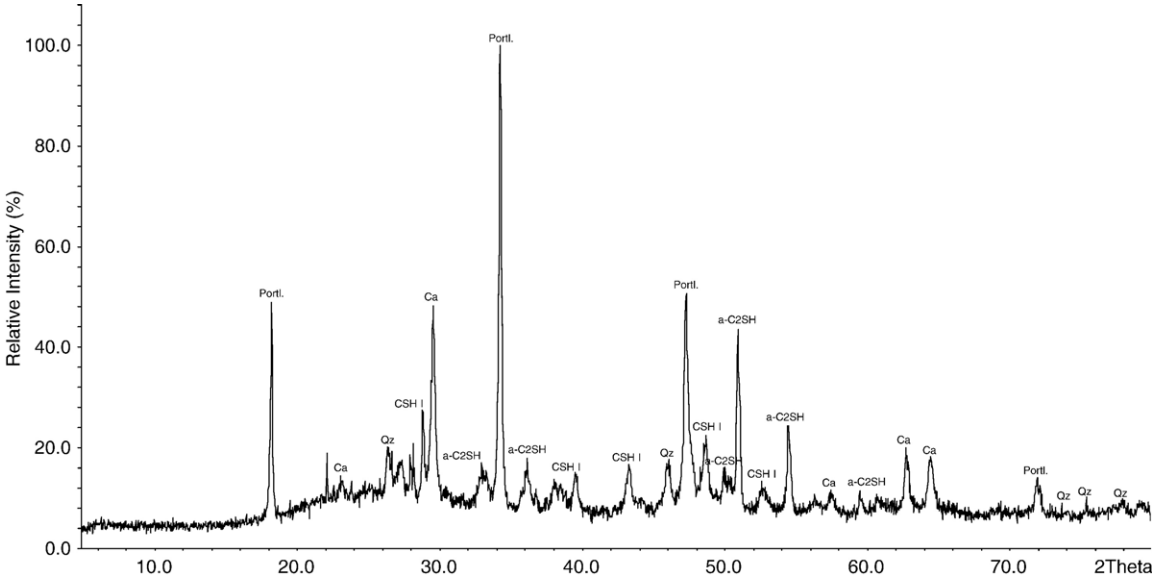

Fig. 26. X-ray powder pattern of the lime sand pellet with raw perlite (C/S = 0.53).

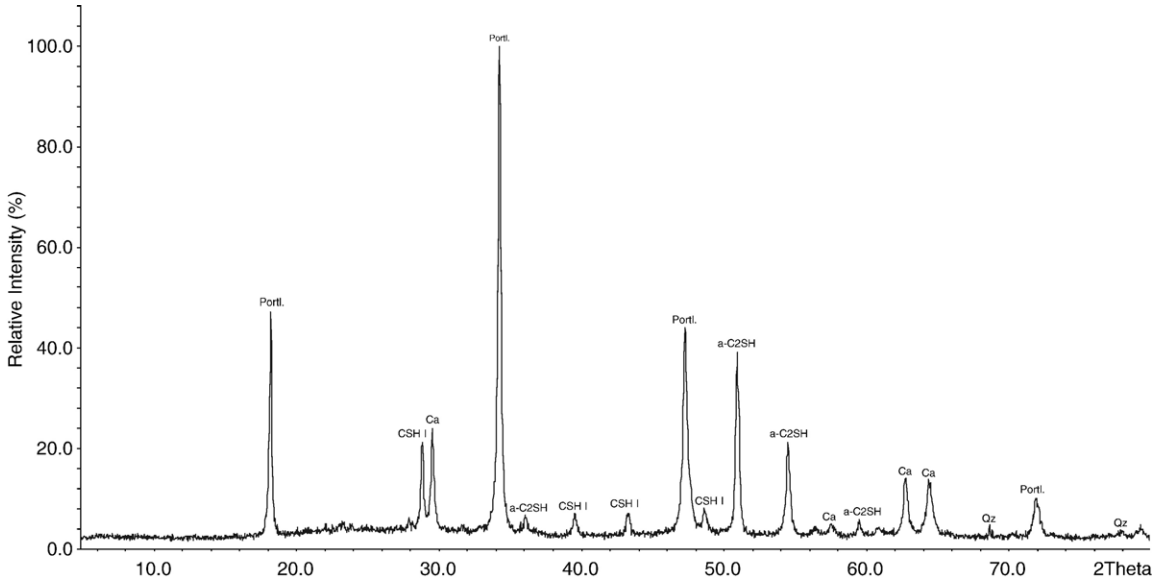

Fig. 27. X-ray powder pattern of the lime sand pellet with raw perlite (C/S=0.83).

sand agree with the results of [9], obtained with powder samples. Using quartz with a grain-size comparable to the material used by [9], the formation of α-C_2SH as a reaction product could be verified as well. In agreement with [9] the results of the present work obtained with lime sand pellets with C/S ratios of 0.53 and 0.83 showed a lime enrichment and residual quartz besides the formation of C–S–H phases in the pellets with quartz sand as silica source. These findings indicate an incomplete conversion of the reactants due to a low reaction rate under the experimental conditions.

Further, in analogy to our former investigations made on powder samples, the present results have shown an increase of the amount of portlandite for the lime sand pellets with quartz sand and a C/S ratio of 0.83.

In the lime sand pellets with quartz powder a wide reaction zone around the quartz grains >10 μm was found for C/S ratios of 0.53 and 0.83. The single quartz crystals were embedded in a matrix of portlandite. Direct contact between the quartz grains could not be observed which agrees with the investigations of [10]. The reaction zone consisted of C–S–H phases, which were developed from a gel substance. According to investigations of [11] this reaction zone can show a width up to ≤20 μm. The crystals developed from gel had a size of ≤2.5 μm. They were partly grown together and showed a fibrous and rod-shaped morphology. The formation of C–S–H phases could be observed only on the side of the $Ca(OH)_2$. This can be explained by the higher mobility of Si in contrast to Ca under autoclave conditions [13]. Whereas a crystallization of 11 Å tobermorite could be expected from literature [6, 12], our X-ray powder data clearly show that only a mixture of CSH I and α-C_2SH was formed besides portlandite and calcite. Future studies on reaction kinetics are necessary to decide, if phase transformation of CSH I and α-C_2SH into 11 Å tobermorite is already in the early stage here [14].

In contrast to the results on pellets X-ray investigations of powder samples with quartz powder confirmed the formation of 11 Å tobermorite for C/S ratios of 0.53 and 0.83 [2]. From this it can be concluded that powder samples favour the formation of 11 Å tobermorite. In the case of lime sand pellets with quartz powder maybe an increase of the hardening time should lead to a higher amount of 11 Å tobermorite.

In the lime sand pellets with inflated clay sand and a C/S ratio of 0.53 and 0.83 the high porosity of the raw single inflated clay grains could be observed. Electron microscopical investigations have shown that an abundant formation of C–S–H phases occurred only for a C/S ratio of 0.53. This agreed with the results for the previously investigated powder samples with inflated clay sand [4]. With the pellets, C–S–H crystals were formed with a size of ≤10 μm, occurring only in big pores of about >20 μm. From the crystal size and the needle-like morphology a formation of xonotlite could be supposed [6, 11]. After [6] a formation of xonotlite especially takes place in big pores. This agrees with the results of the present work. According to [8] the formation of xonotlite indicates the termination of C–S–H phase formation and marks the highest possible stability of lime sand products. But because xonotlite mainly occurs in big pores it has no major influence on the stability of lime sand products. Our X-ray investigations on the lime sand pellets with inflated clay sand and a C/S ratio of 0.53 also revealed a formation of xonotlite besides 11 Å tobermorite. At a C/S ratio of 0.83 no formation of 11 Å tobermorite could be identified. This agrees with the results obtained for the powder samples as 11 Å tobermorite was found only for a C/S ratio of

Table 4
Values of pore area [m^2/g], pore diameter [μm] and porosity [%] of selected lime sand pellets (C/S=0.53)

Silica source	Pore area [m^2/g]	Pore diameter [μm]	Porosity [%]
Quartz powder	6451	0.0338	7.96
Quartz sand	4114	0.0641	6.48
Inflated clay sand	38,574	0.0136	21.92
Raw perlite	5075	0.0449	6.59

0.53 [4]. In the lime sand pellets with a C/S ratio of 0.83 only small amounts of xonotlite could be detected. This agrees with the results of the ESEM investigations.

The reaction behaviour of the lime sand pellets with raw perlite was significantly different to the results described so far. The ESEM investigation showed no formation of C–S–H crystallites, irrespective of the C/S ratio. In contrast X-ray analysis revealed α-C_2SH, C–S–H (I), portlandite and calcite as synthesis products. This difference is assumed to be a result of the only very small crystal size of the C–S–H phases. According to [1] the formation of α-C_2SH takes place preferentially at vacancies on the quartz surface. Because of the high grain-size of ≤1 mm, a smooth surface and low specific surface area of 0.14 m^2/g an abundant formation of C–S–H phases could not be expected. In analogy to the powder samples with raw perlite investigated previously [4], the lime sand pellets with raw perlite also showed no formation of 11 Å tobermorite with C/S-ratios of 0.53 and 0.83.

5. Conclusions

Our experimental study shows that in the case of the lime sand pellets with quartz sand, quartz powder and inflated clay sand a formation of C–S–H phases could be confirmed, but 11 Å tobermorite could be verified only for inflated clay sand.

For the industrial production of lime sand products the investigations on alternative silica sources described here could be utilizable.

Because C–S–H phase formation is a reaction controlled by kinetics, phase formation, reaction velocity and total conversion of the reactants showed certain differences, when lime sand pellets were used instead of powder samples. To increase the yield of C–S–H phases from pellets an increasing reaction time has to be tested first of all.

Our experiments also revealed that ESEM in combination with XRD is a versatile tool for phase characterizations within complicated reaction systems.

References

[1] H. Mörtel, Mineralbestand, Gefuege und physikalische Eigenschaften von Kalksandsteinen, Fortschr. Mineral. 58 (1) (1980) 37–67.
[2] A. Hartmann, J.Ch. Buhl, Untersuchungen zur Kristallisation von 11 Å Tobermorit in Abhaengigkeit von den Reaktionsbedingungen, Z. Kristallogr. (Supple 19) (2002) 86.
[3] A. Hartmann, J.Ch. Buhl, Untersuchungen zur Kristallisation von 11 Å Tobermorit in Abhaengigkeit von den Reaktionsbedingungen, Beih. Eur. J. Mineral. 14 (1) (2002) 63.
[4] A. Hartmann, J.Ch. Buhl, Alternative Siliziumquellen zur Kristallisation von 11 Å Tobermorit, Z. Kristallogr. (Supple 20) (2003) 97.
[5] A. Hartmann, J.Ch. Buhl, Ch.F. Hendriks, Gefuege-und Phasenuntersuchungen zur Kristallisation von 11 Å Tobermorit in Kalksilikat-Presslingen, GDCh Bauchemie, Kurzreferate, ISBN: 3-936028-11-7, 2003, p. 22.
[6] H. Mörtel, Die Gefuegeentwicklung der CSH-Phasen in Kalksandsteinen im Temperaturbereich von 120–250 °C bei Haltezeiten von 1/2 Stunde-2 Wochen, Folgerungen fuer die Eigenschaften von Kalksilikatprodukten. Internationales Symposium ueber die Beziehungen zwischen den Eigenschaften von KS-Produkten und dem Bindemittelaufbau, Karlsruhe, 1978.
[7] H.E. Schwiete, G. Rehfeld, Gefuegeuntersuchungen an dampfgehaerteten Baustoffen mit Hilfe des Rasterelektronenmikroskops. 2, Internationales Symposium fuer Dampfgehaertete Kalziumsilikat-Baustoffe, Hannover, 1969.
[8] F. Kendel, Die Entwicklung des Bindemittelaufbaus von KS-Produkten in Abhaengigkeit von Haertetemperatur und –zeit, Auswirkungen auf die mechanischen Eigenschaften. Internationales Symposium ueber die Beziehungen zwischen den Eigenschaften von KS-Produkten und dem Bindemittelaufbau, Karlsruhe, 1978.
[9] Aghmaghani-Esmail, Die hydrothermale Kristallisation von Tobermorit und tobermoritaehnlichen Phasen, Diplomarbeit, Institut fuer Mineralogie der Universitaet Hannover, 1977.
[10] W. Eden, J.Ch. Buhl, Herstellparameter von Kalksand-Spezialbaustoffen fuer die Abschwaechung von Waermebruecken im Mauerwerksbau, Forschungsvereinigung Kalk-Sand e.V., Forschungsbericht, 92, 2002.
[11] V. Lach, Untersuchungen der Mikrostruktur wasserdampfgehaerteter Kalksandsteine, Internationales Symposium ueber die Beziehungen zwischen den Eigenschaften von KS-Produkten und dem Bindemittelaufbau, Karsruhe, 1978.
[12] M. Matwejew, M. Nikolajewa, Beitrag zur Kristallchemie der Hydratationsprozesse mineralischer Bindemittel, Silikattechnik 32 (6) (1981) 167–169.
[13] T.J. Peters, et al., Vergleichende Untersuchungen ueber das Verhalten von quarzarmem, glazialem Sand und reinem Quarzsand fuer die Herstellung von Kalksandstein und Glasbeton mit besonderer Berueksichtigung des Reaktionsmechanismus, Internationales Symposium ueber die Beziehungen zwischen den Eigenschaften von KS-Produkten und dem Bindemittelaufbau, Karlsruhe, 1978.
[14] R. Kondo, Kinetische Studien ueber die hydrothermale Reaktion zwischen Kalk und Kieselsaeure, Internationales Symposium fuer damphgehaertete Baustoffe, London, 1965.